

Change in the Orientation and Packing upon Adsorption of Pyranine Molecules onto Cationic Langmuir Monolayers and Langmuir–Blodgett Films

Osamu Tsukamoto, Masumi Villeneuve, Akira Sakamoto, and Hiroo Nakahara*

Department of Chemistry, Faculty of Science, Saitama University, 255 Shimo-Okubo, Sakura-ku, Saitama 338-8570

Received November 22, 2006; E-mail: nakahara@chem.saitama-u.ac.jp

Differrent adsorption behaviors and the orientation of pyranine molecules were investigated for the cationic Langmuir monolayers by using Brewster angle microscopy (BAM), two-dimensional (2D) phase behavior with elasticitic property of the monolayers and in situ visible spectroscopy. The structural change in the cationic Langmuir–Blodgett (LB) films before and after adsorbing pyranine molecules was found by using small angle and in-plane XRD. The excited-state proton-transfer (ESPT) between octadecylamine (ODA) and pyranine adsorbed in the films was investigated using time-resolved fluorescence spectroscopy together with consideration of the film structures.

Molecular-organized systems have attracted much attention in the application of electronic and optical devices.[1] Control of the molecular orientation and packing is expected to provide valuable information for constructing novel molecular devices. The Langmuir–Blodgett (LB) method is a good method for controlling the molecular arrangements.[2]

Adsorption of functional dyes onto LB films is a unique technique to immobilize functional dyes in organized molecular (LB) films, which mainly occurs via ionic interactions between a film substance and dye molecules. Cationic film substances interact with various anionic functional dyes,[3] proteins,[4] and nano particles.[5] Previously, the adsorption behavior of several dye molecules, such as azo dye,[6] alizarine violet,[7] and sulforhodamine B,[8] onto cationic LB films have been reported. The molecular arrangements of functional dyes in the highly ordered LB assemblies depend on the adsorption conditions, such as aqueous pH, dye concentrations, and a temperature, in addition to the position of the substituent functional groups as well as compositions and structures of the cationic LB films.

Pyranine (8-hydroxy-1,3,6-pyrenetrisulfonic acid trisodium salt) is a typical hydroxyarene, and it is known that its acidity is increased in the excited state and causes excited-state proton-transfer (ESPT) in polar solvents.[9,10] In a previous paper, Ray and Nakahara have reported the ESPT process in pyranine-adsorbed octadecylamine LB films.[11] In the present work, in order to investigate effects of the different molecular packings and orientation of cationic amphiphiles on dye adsorption and ESPT in the LB film, several cationic films, such as *n*-octadecylamine (ODA), a gemini amphiphilic ammonium salt having two alkyl chains, and their mixtures, were studied. The adsorption behavior at the air/water interface and the 2D arrangements of pyranine onto the cationic Langmuir monolayers were examined by analyzing surface pressure-area (π–A) isotherms, Brewster angle microscopic (BAM) images and in situ visible spectra. The pyranine molecules take different aggregates in the films in accordance with the phase behavior of the monolayers. The obtained spectral shifts, in comparison with the solution spectra, were analyzed with an exciton model due to the strong dipole–dipole interaction between the pyranine molecules in the 2D arrangements. The BAM images of the monolayers were similar to the in situ visible spectra. These transferred films were characterized by UV–vis absorption and fluorescence spectra, and out of plane and in-plane X-ray diffraction (XRD). In addition, the ESPT reaction in the dye-adsorbed LB films was investigated by using time-resolved spectroscopy.

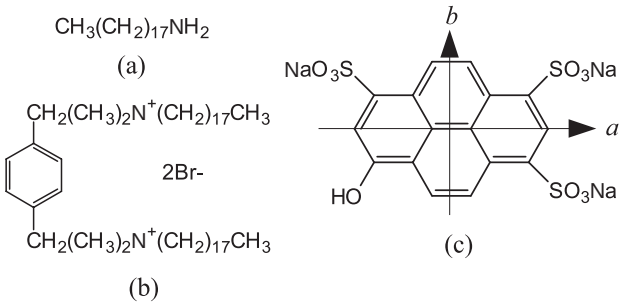

Fig. 1. Structural formulas of the ODA (a), *p*-PODB (b), and pyranine (c).

Experimental

Cationic amphiphiles and the dye used in this work are shown in Fig. 1. Octadecylamine (**a**: ODA) was purchased from Aldrich Co., Ltd. and recrystallized five times from a hexane solution. The dialkyl amphiphile *p*-phenylenedimethylenebis(octadecyldimethylammonium) dibromide (**b**: *p*-PODB) was synthesized according to the literature.[12] Pyranine was purchased from Acros Ltd. and was used as recieved, and the purity was checked with UV–visible absorption spectroscopy.[10]

The cationic monolayers were spread from a chloroform solution onto an alkaline aqueous subphase (NaOHaq, pH $\approx$10, 20.0 °C) with and without pyranine (1×10^{-4} mol L^{-1}). The distilled water was deionized by using a Milli-Q Plus (resistivity:

Published on the web September 13, 2007; doi:10.1246/bcsj.80.1723

18.2 MΩ cm). Surface pressure–area (π–A) isotherms of the monolayers were measured by a film balance (Langmuir–Adam type, FW-2, LAUDA), and the phase behavior of the monolayers was determined with the film elasticity defined by the following:[13]

$$E_s = -A(\partial\pi/\partial A)_T, \quad (1)$$

where A is the molecular area and π is the surface pressure. In situ visible spectra of the Langmuir monolayers adsorbed pyranine molecules were measured by using a spectrometer with a multichannel photodetecter (MCPD-100, Otsuka Electronics Co., Ltd.). In situ observation of the monolayer morphology was performed by using a Brewster angle microscopy (BAM) (EP^3, NFT Co.,), which was equipped with a 20 mW semiconductor laser (λ = 532 nm), an analyzer and a zooming microscope with a highly sensitive CCD camera. The scale of BAM images was 486 μm × 384 μm. The Langmuir monolayers were transferred onto the solid substrates at 25 mN m^{-1} and 20 °C by using the Langmuir–Blodgett method. The dipping rate was 7 mm min^{-1} for both up and down strokes to give an alternating Y-type film. Cleaned Quartz plates were used for UV–vis absorption and fluorescence spectroscopies, and hydrophobilized glass plates were used for XRD studies. Absorption and fluorescence spectra were recorded on UV–vis absorption (U-3210, Hitachi) and fluorescence (Jasco, FP-6300) spectrophotometers, respectively. Time-resolved fluorescence spectra were measured by using a streak camera. The fundamental output (wavelength 775 nm, pulse width ≈ 130 fs, repetition rate 1 kHz) from a femtosecond Ti:Sapphire (1550 nm) regenerative amplifier seeded by the second harmonic of a mode-locked Er-doped fiber laser (Clark-MXR, CPA-2000) was used to excite an optical parameteric amplifier (Clark-MXR, IR-OPA). The signal wave (wavelength 390 nm) from the optical parametric amplifier was used to excite the sample. The laser beam was focused on the film sample in a quartz cell under a nitrogen atmosphere. Scattered light at 90° to laser beam was collected and focused onto the entrance slit of a single spectrograph (Acton Research, SpectraPro 150). Filters were placed between the collimate lens and the entrance slit. A streak camera (Hamamatsu, C4334-01) was attached to the output port of the spectrograph and operated with the synchronous delay generator (Hamamatsu, C4792-01) to compensate for the time delay in the electronic circuit of the streak camera. The two-dimensional data from the streak camera were accumulated and analyzed with a personal computer in a photocounting mode. The full width at half maximum (FWHM) of the instrument response function was about 30 ps. To examine of the excited-state dynamics of LB films, the fluorescence decays were measured at 440 and 510 nm. A fluorescence decay curve was fitted to multi-exponential functions deconvoluted with the instrumental response function, giving a weighted mean fluorescence lifetime. Small angle (out of plane) X-ray diffraction was measured by a Rigaku Rad-B X-ray diffractometer equipped with a graphite monochromator (Cu Kα radiation, 40 kV, 30 mA) to obtain the long-spacing of the LB film. The in-plane lattice structure of the LB film was determined by the grazing X-ray incidence at 0.2° with a parabolic graded multilayer mirror to obtain molecular level resolution (Bruker AXS, MXP-BX, Cu Kα radiation, 40 kV, 40 mA).

Results and Discussion

Figure 2a shows π–A isotherms of the monolayers for ODA, *p*-PODB and a 2:1 mixture of ODA:*p*-PODB (ODA:*p*-PODB = 2:1) on the NaOHaq (pH 10) at 20.0 °C, as compared with those containing pyranine molecules (1×10^{-4} mol L^{-1}, pH 10), as shown in Fig. 2b. In addition, for these monolayers on the NaOHaq with or without the dye molecules, changes in the film elasticity vs. the surface pressure are indicated in Fig. 3. From the curves for ODA (a) and for *p*-PODB (c) in Fig. 3, the former monolayer exhibited a typical solid-condensed film, and the latter monolayer formed only a liquid-expanded film. This behavior agrees with the previous works.[8,12,14] Alternatively, in the case of their mixed monolayer (ODA:*p*-PODB = 2:1), three phases appeared depending on the surface pressure, as shown with curve (b) in Fig. 3. The liquid-expanded phase was in the range of a few to 17 mN m^{-1}, in which its elasticity is nearly equal to that of the *p*-PODB monolayer. When the mixed monolayer was compressed above 27 mN m^{-1}, the monolayer seemed to be a mesophase in the region of 27–37 mN m^{-1}. As well, a liquid-condensed monolayer was obtained at pressures above 40 mN m^{-1}. Since the mixed monolayer gave a rather negative deviation from the presumably ideal mixing in the plot of the molecular area vs. the composition and the continuous increase in the collapsed pressure, though the *p*-PODB mono-

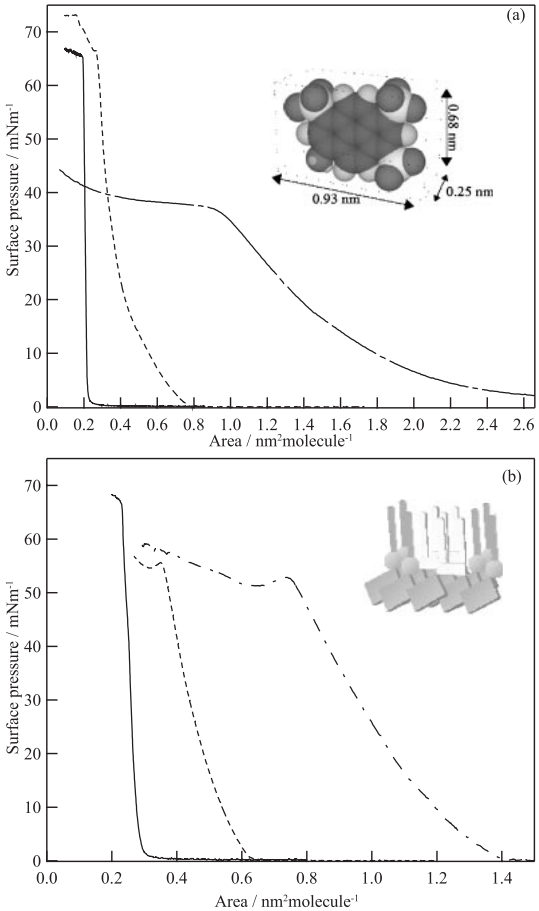

Fig. 2. Surface pressure–area (π–A) isotherms of ODA (solid line), ODA:*p*-PODB = 2:1 (dotted), and *p*-PODB (dot-dashed) in NaOHaq at pH 10 (a) and 1×10^{-4} mol L^{-1} pyranine NaOHaq (b) at 20 °C. Inset shows the molecular dimension of pyranine structure (a) and the orientation manner of the ODA:*p*-PODB = 2:1 Langmuir monolayer on 1×10^{-4} mol L^{-1} pyranine NaOHaq (b).

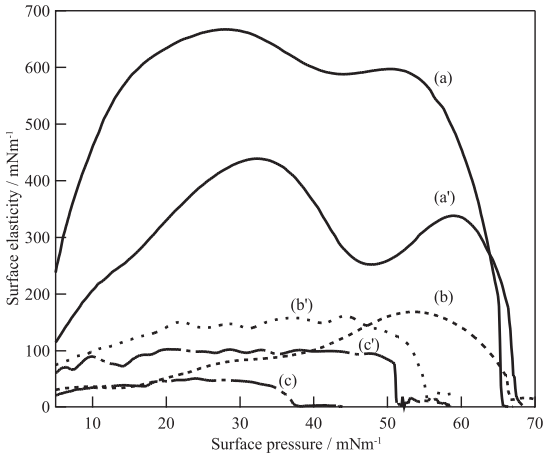

Fig. 3. Surface elasticity vs. surface pressure of ODA (**a**, solid line), ODA:*p*-PODB = 2:1 (**b**, dotted), and *p*-PODB (**c**, dot-dashed) on NaOHaq (a, b, c) and 1×10^{-4} mol L^{-1} pyranine NaOHaq (a′, b′, c′) at pH 10 and 20 °C.

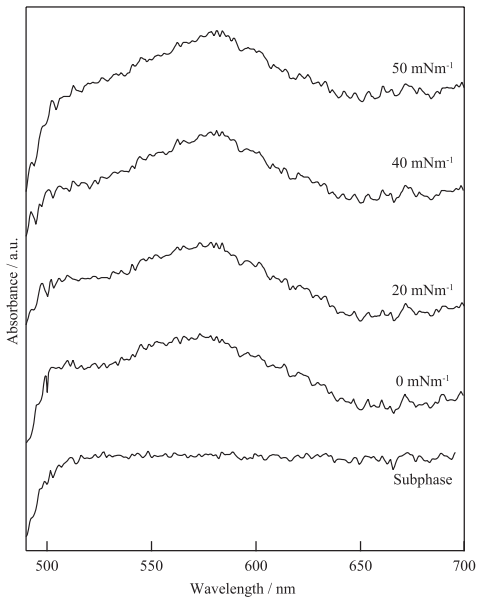

Fig. 4. In situ visible spectra of pyranine molecules adsorbed onto ODA:*p*-PODB = 2:1 Langmuir monolayers.

layer collapsed at around 37 mN m^{-1}, the ODA and *p*-PODB molecules appeared to be miscible in the monolayer, and the ODA molecules seemed to be organized in a space-filling manner between the two alkyl chains of *p*-PODB. These facts are thought to correspond to the rigidity of the *p*-PODB monolayer, which is increased by mixing. A similar interaction between ODA and *p*-PODB was observed in the mixed monolayer in the other compositions.

When the monolayers were spread on the pyranine NaOH aqeous solution, the π–*A* isotherms changed considerably, depending on the kinds of cationic films. As shown in the inset of Fig. 2a, the cross-sectional area of a pyranine molecule were estimated using a CPK model in which the molecular dimensions were estimated to be 0.93 and 0.68 nm along the long (*a*) and the short (*b*) axis of pyranine, respectively, to be 0.23 nm^2 for the side-on and 0.63 nm^2 for the flat-wise orientation. The molecular area in the monolayer of ODA changed from 0.21 to 0.26 nm^2 at 25 mN m^{-1} upon adsorption the pyranine molecules. This behavior suggests the formation of an ionic complex between the cationic film substances and the pyranine molecules. In the case of the insertion of the pyranine molecules into the ODA monolayers, the expansion of molecular area was rather small on account of molecular size of the pyranine. Therefore, it is suggested that one pyranine molecule seems to be loosely packed lying under the monolayer of one or three ODA molecules. However, the molecular area in the case of the *p*-PODB monolayer adsorbed pyranine molecules is significantly reduced from 1.2 to 1.0 nm^2 at 25 mN m^{-1}. From the film elasticity of the *p*-PODB monolayer adsorbed pyranine molecules, the monolayer is more rigid as compared with that before adsorption. This fact indicates that the *p*-PODB monolayer is considered to immobilize the dyes, leading a well-fitted molecular packing of both molecules. In the ODA:*p*-PODB = 2:1 mixed monolayer with adsorbed pyranine molecules, the molecular area increased from 0.39 to 0.46 nm^2 upon adsorption at 25 mN m^{-1}. The expanded molecular area (0.07 nm^2) suggests that two or three of the film molecules adsorb the pyranine molecules, which have a fairly tilted conformation in the mixed monolayer as shown in the inset of Fig. 2b. These changes of the molecular orientation seems to be reflected, in the electronic spectra of the film adsorbed pyranine.

Figure 4 shows in situ visible spectra of the ODA:*p*-PODB = 2:1 mixed monolayer at various surface pressures, immediately after adsorption of the pyranine molecules. After spreading the mixed monolayer, an additional peak and a shoulder appeared at 572 and 502 nm, respectively, whereas the peak at 460 nm for the pyranine monomer in the aqueous solution at pH 10 reduced remarkably. The larger red-shifted bands are thought to be the two-dimensional aggregates of pyranine by adsorption under the monolayer. In general, the spectral shift can be explained with the exciton coupling theory, due to the dipole–dipole interaction between the neighboring molecules in the two-dimensional array.[15] For the linear dye aggregate in the monolayer, the spectral shift is expressed as:

$$\Delta\nu = \frac{2}{hc}\frac{(N-1)}{N}\frac{\mu^2}{r^3}(1-3\cos^2\alpha), \qquad (2)$$

where $\Delta\nu$ is the spectral shift in wavenumber from the monomer, *h* is Planck's constant, *c* is the velocity of light, *N* is the number of molecules in the aggregate, *r* is the distance between the molecular centers, and α is the angle between the dipole moment of the molecule and the line through the center of molecules in the two-dimensional aggregate. For example, it is well known that cyanine dye to form the J-aggregate with a red-shifted band or the H-aggregate with a blue-shifted.[16,17] In accordance with Eq. 2, the red shift in the spectra from the monomer to the aggregates suggests a rather parallel orientation of the long axis of the pyranine molecules in the head-to-tail array. With an increase in the surface pressure, the relative intensity of the band around 570 nm increased and shifted slightly to the longer wavelengths (570–580 nm), and the shoulder band around 503 nm at zero surface pressure decreased at 20 mN m^{-1} and disappeared at 40–50 mN m^{-1}. These spectral changes are related to the different molecular

arrangements for the dye aggregates in the monolayer through the compression. The molecular microenvironments and packing can be attributed to the monolayer elasticity. Accompanied with these spectral shifts, the film elasticity increased to be nearly 150 mN m^{-1} at the surface pressure of 20 mN m^{-1} as shown in Fig. 3, indicating a phase transition from the gas- or liquid-expanded phase to the liquid-condensed phase. In addition further compression induced the disappearance of the shoulder band at 503 nm. As a result, this spectral change for the pyranine molecules adsorbed under the mixed monolayer corresponds to the phase transition. For the pyranine molecules adsorbed ODA and *p*-PODB monolayers, the bands also appeared at 570 and 550 nm respectively. The shoulder band at 503 nm was not observed, and the spectra did not change with the surface pressure.

BAM image provided further information about the film behavior upon dye adsorption in terms of the monolayer morphology. The ODA monolayer gave a solid-condensed domain due to the film rigidity, whereas the *p*-PODB did not show any clear domain for its fluid film. In the ODA:*p*-PODB = 2:1 mixed monolayer, a small crystalline region appeared only at surface pressures above 10 mN m^{-1}, which suggests that these monolayers do not easily crystallize. The BAM images of the NaOHaq subphase containing pyranine (1×10^{-4} mol L^{-1}) at 20 °C showed uniform and homogeneous structures upon adsorption of the pyranine molecules. The BAM images of the ODA, ODA:*p*-PODB = 2:1, and *p*-PODB monolayers at 0 and 25 mN m^{-1} are shown in Fig. 5. Even at 0 mN m^{-1}, as shown in Fig. 5A, different structures were obtained for the ODA, *p*-PODB, and their mixed monolayers adsorbed the pyranine molecules. A rigid condensed film with clear edge-like domains for the ODA was observed irrespective of the adsorption of pyranine molecules. The fluid-expanded film with unique network domains, like an arabesque for the *p*-PODB and the amorphous structure containing the expanded and the condensed phases for the mixed film, were obtained by introducing the pyranine molecules. In Fig. 5B at 25 mN m^{-1}, large domains with less defects for the ODA and homogeneous domains for *p*-PODB and the mixed monolayer appeared.

Figure 6 shows UV–vis absorption spectra of the pyranine-adsorbed Langmuir–Blodgett films (21 layers) of ODA, ODA:*p*-PODB = 2:1 and *p*-PODB transferred at 25 mN m^{-1}. The bands at 370 and 405 nm were attributed to S_0–^1L_a and S_0–^1L_b transiton for the protonated species (PyOH), respectively. However, the band at the 460 nm was assigned to S_0–S_1 transition for the deprotonated species (PyO^-).[10] The spectral shift in the deprotonated band (S_0–S_1 transition) of the deposited film was smaller than that of Langmuir monolayers, and protonated bands were observed. Based on the literature,[1,18,19] it is plausible for the molecular orientation and packing to change slightly through deposition. It is possible that rearrangement of the pyranine aggregates and protonation of pyranine occur during deposition of the Langmuir monolayer adsorbed dyes and the drying process. The transition moments in the aromatic ring were observed to be lying rather flat in an anisotropic orientation from the polarized visible spectra.

XRD measurements were carried out in order to examine the film structure with and without adsorption of pyranine

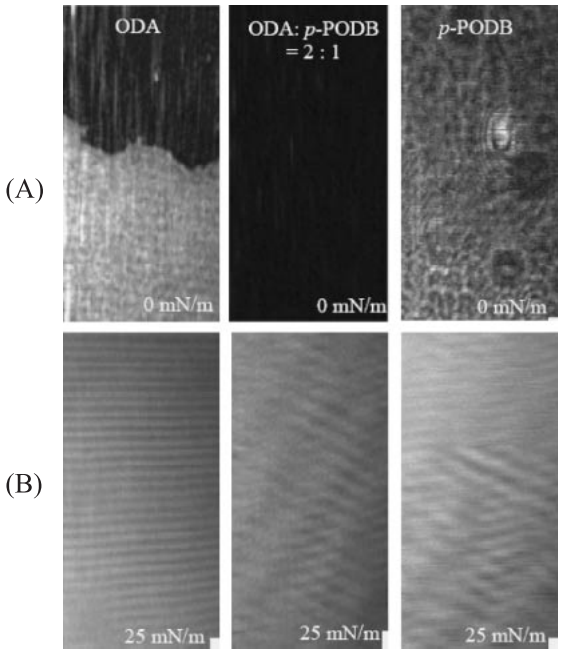

Fig. 5. BAM images of ODA, ODA:*p*-PODB = 2:1, and *p*-PODB monolayer on 1×10^{-4} mol L^{-1} pyranine NaOHaq at 0 mN m^{-1} (A) and 25 mN m^{-1} (B) (size: 200 μm × 100 μm).

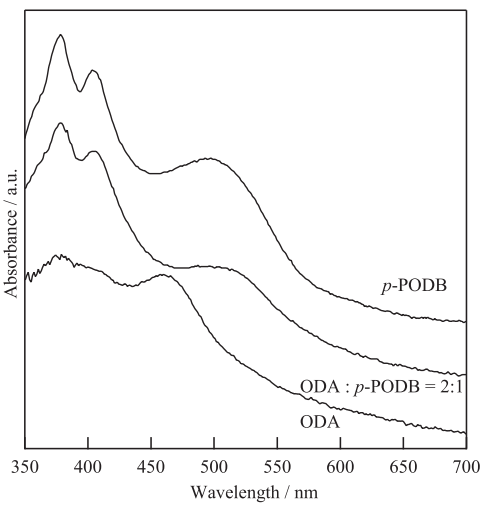

Fig. 6. UV–vis absorption spectra of pyranine-adsorbed ODA, ODA:*p*-PODB = 2:1, and *p*-PODB LB films (21 layers).

molecules onto the ODA, ODA:*p*-PODB = 2:1, and *p*-PODB LB film deposited at 25 mN m^{-1}. Figure 7 shows the small angle and in-plane XRD profiles of the cationic LB films (A) and pyranine-adsorbed films (B). In the ODA system, the layer-by-layer distance (d_l) of the pyranine-adsorbed LB film (5.52 nm) from the diffraction peaks at $2\theta = 4.76°$ ($n = 3$, 1.84 nm) was longer than that without the dye (5.25 nm) from the diffraction peaks at $2\theta = 5.04°$ ($n = 3$, 1.75 nm). These values indicate a bilayer thickness. It is suggested that the increase in the thickness is due to the thickness of the flat-wise configuration of the pyranine molecules sandwiched by the ODA molecules (0.27 nm) in addition to change in

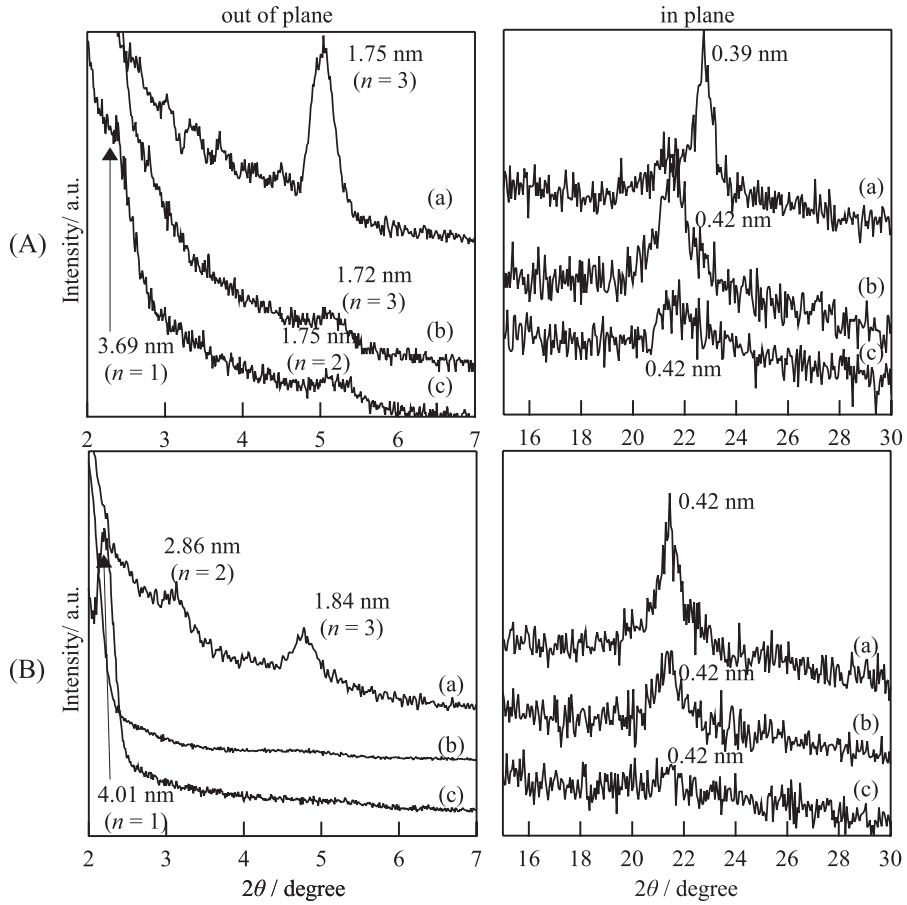

Fig. 7. Small angle (left hand side) and in-plane XRD (right hand side) profile of ODA (a), ODA:*p*-PODB = 2:1 (b), and *p*-PODB (c) LB films (A) and those films with adsorbed pyranine (B).

the molecular orientation. In the case of the ODA:*p*-PODB = 2:1 and *p*-PODB LB films, the layer-by-layer distance (d_l) obtained from the diffraction peaks at $2\theta = 5.12^\circ$ ($n = 3$, 1.72 nm) and 2.39° ($n = 1$), were 5.16 and 3.69 nm, respectively. Assuming that the fully stretched length of ODA and *p*-PODB are 2.4 and 2.6 nm, respectively, the obtained long spacing distance of these LB films are shorter than the bilayer thickness. Therefore, it is suggested that the bilayer film takes an interdigitated structure and/or somewhat inclined in the ODA:*p*-PODB = 2:1 and *p*-PODB LB films without adsorbing the dye. The overlapping part of the ODA:*p*-PODB = 2:1 and *p*-PODB LB films are estimated to be 0.04 and 1.70 nm. For the ODA:*p*-PODB = 2:1 mixed film adsorbed pyranine molecules, the diffraction peak were reduced or disappeared. On the other hand, a clear diffraction peak at $2\theta = 2.20^\circ$ was observed for the pyranine-adsorbed *p*-PODB LB film, which indicates d_l is 4.01 nm. The shift of 0.32 nm after adsorbing the dye suggests that a structural change in the LB film within the bilayer.

In-plane XRD was performed to investigate the difference in the alkyl-chain packing due to the dye adsorption, as shown in the right hand sides of Fig. 7. For the ODA system, the alkyl-chain packing was a slightly distorted orthorhombic lattice (0.39 and 0.42 nm) and changed to an isotopic hexagonal lattice (0.42 nm) upon adsorption of the pyranine molecules. These results suggest that rearrangement of the alkyl-chain packing in the ODA LB film occurrs during adsorbing pyranine molecules. The ODA:*p*-PODB = 2:1 and the *p*-PODB LB films exhibited only a single peak at $d_{in} = 0.42$ nm, which suggests isotropic hexagonal sub-cell packing. This value did not change upon adsorption of the dye though the diffraction intensity was reduced. This result suggests that two-dimensional spacing ($d_{in} = 0.42$ nm) provides sufficient distance for adsorbing the pyranine molecules into the cationic LB film.

Figure 8 shows the fluorescence spectra of the pyranine-adsorbed LB films excited by 390 nm. From the analysis of the aqeous solution's spectra, the band at 440 nm could be attributed to protonated species ($PyOH^*$), and the band at 510 nm was ascribed to deprotonated species (PyO^{-*}).[10] The emission band of the deprotonated dye could be due to the excited-state proton-transfer between an amino group of octadecylamine and hydroxy group of pyranine. The protonation and deprotonation kinetics of hydroxyarenes are very sensitive to the proton acceptor. So, the peak intensities at 445 and 510 nm strongly depend on the compositions of mixed cationic LB film. From the fact that *p*-PODB cannot be a proton acceptor, as the mixing ratio of *p*-PODB was increased, the band intensity at 440 nm decreased. Whereas the deprotonated band was observed in the spectrum of the *p*-PODB LB film with adsorbed pyranine molecules. This can be ascribed to H_2O molecules incorporated in the LB film during the deposition. The emission band intensity around 580 nm band changed with

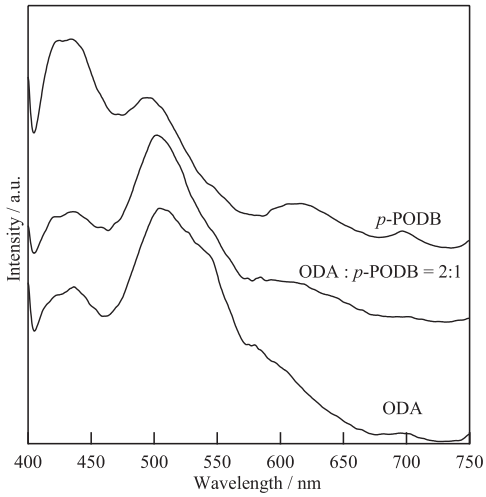

Fig. 8. Fluorescence spectra of pyranine-adsorbed ODA, ODA:*p*-PODB = 2:1 and *p*-PODB LB films (21 layers) excited at 390 nm.

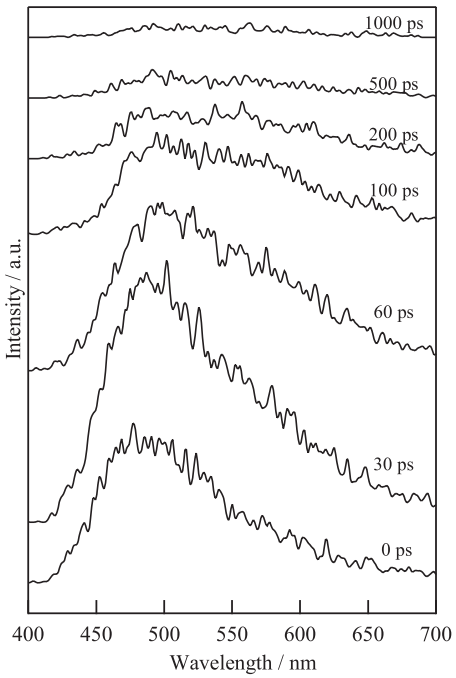

Fig. 9. Time-resolved fluorescence spectra of ODA:*p*-PODB = 2:1 LB film (21 layers).

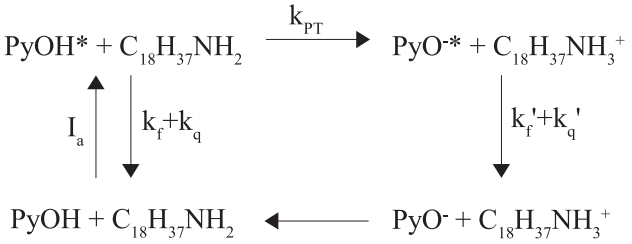

Scheme 1.

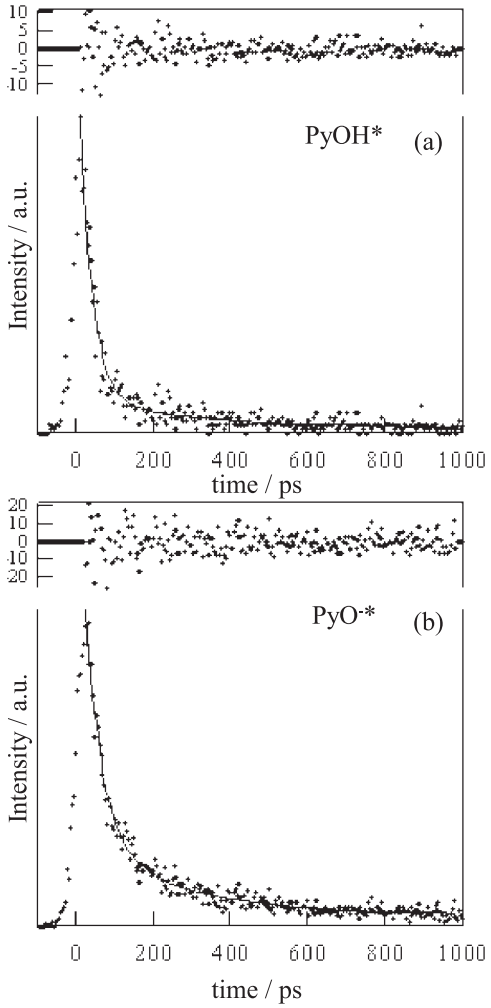

Fig. 10. Fluorescence decay and double-exponential fitting curve of ODA:*p*-PODB = 2:1 LB film (21 layers) at (a) 440 nm and (b) 500 nm.

the film substances, suggesting formation of excimers. In an excimer, face to face interaction for pyranine depends on the film structure composed of ODA, *p*-PODB, and their mixture. This result is supported by the time-resolved fluorescence spectra (Fig. 9).

In addition, effects of the molecular arrangement of pyranine molecules on the dynamics of the excited-state proton-transfer were studied by the time-resolved fluorescence spectroscopy. Based on the Förster cycle,[20] the ESPT kinetics in the pyranine-adsorbed film has described by Scheme 1,[21,22] in which k_{PT} is the rate constant of the proton transfer to the octadecylamine from the pyranine molecules, k_f and k_q are radiative and non-radiative rate constants of the PyOH*, respectively, and k_f' and k_q' are radiative and non-radiative rate constants of the $PyO^{-}*$, respectively.

Figure 9 shows the time-resolved fluorescence spectra of an ODA:*p*-PODB = 2:1 mixed LB film with adsorbed pyranine molecules. The emssions of the protonated and deprotonated species show very rapid decay in comparison to the case of an aqueous solution (lifetime = 5.6 ns), accompanied with a delayed emission due to the excimer around 580 nm. Figure 10 shows the fluorescence decays of the ODA:*p*-PODB = 2:1

Table 1. Relative Fluorescence Quantum Yield Ratio (Φ'/Φ), Decay Parameter (τ_i, α_i), and Proton-Transfer Rate Constant (k_{PT}) of ODA, ODA:*p*-PODB = 2:1, and *p*-PODB LB Films (21 Layers) with Adsorbed Pyranine Molecules

Sample	Φ'/Φ		Fluorescence life time		k_{PT}/s^{-1}
Aqeous solution			440 nm: 4.1 ns, 500 nm: 5.9 ns		4.2×10^{9} a)
Pyranine adsorbed film			τ_1/ps (α_1/%)	τ_2/ps (α_2/%)	
ODA	0.85	440 nm	27.9 (88.9)	194.3 (11.1)	1.77×10^{10}
		500 nm	48.0 (87.9)	231.4 (12.6)	
ODA:*p*-PODB = 2:1	2.54	440 nm	34.1 (92.1)	461.2 (7.9)	4.29×10^{10}
		500 nm	48.9 (84.3)	302.4 (15.7)	
p-PODB	1.86	440 nm	51.3 (89.4)	371.7 (10.6)	2.11×10^{10}
		500 nm	53.2 (77.1)	373.6 (22.9)	

a) This value was noted in the Ref. 29.

mixed LB film with adsorbed pyranine molecules in the region of the protonated (a) and deprotonated (b) bands. According to the previous reports, fluorescence decay curves can be deconvoluted by multi-exponential functions.[23–25] The present fluorescence decay curves could be analyzed as a sum of two exponentials, assuming a compartmental distribution of the aggregate and monomer in the LB film instead of a distribution of the various aggregation types.[26,27] The fluorescence decay profiles are fitted with the following equation:

$$I(t) = \alpha_1 \exp(-t/\tau_1) + \alpha_2 \exp(-t/\tau_2), \quad (3)$$

where $I(t)$ is the fluorescence intensity, τ_i is the fluorescence lifetime, and α_i represents each relative contribution. As shown in Fig. 10, the decay data could be fitted with the two exponential terms. The fluorescence lifetimes of the pyranine-adsorbed ODA:*p*-PODB = 2:1 mixed LB film at 440 nm are 34.1 and 461.2 ps by using Eq. 3. The contributions of the fast and slow components, which amount to $\alpha_1/(\alpha_1 + \alpha_2)$ and $\alpha_2/(\alpha_1 + \alpha_2)$, equal 92.1 and 7.9%, respectively. The siginificantly shorter lifetime of 34.1 ps can be ascribed to the effect of the molecular orientation of the dye on the relaxation process in excited state, though the relatively slow residue component is probably due to some defects in the 2D aggregates. The fluorescence lifetimes at 500 nm were 48.9 and 302.4 ps with the relative contributions of 84.3 and 15.7%, respectively. The fluorescence lifetimes for the other films including the other composition are summarized in Table 1, together with the values of relative fluorescence quantum yields ratio (Φ'/Φ) and k_{PT}. It was found that the composition of cationic LB film affects the fluorescence lifetime. On the account of the film structure as described before, the ODA LB film with adsorbed pyranine molecules with a more uniform structure extremly shorten the fluorescence lifetimes for both the protonated and deprotonated species. In the case of *p*-PODB LB film wiht adsorbed pyranine molecules with a rough surface, a somewhat longer lifetime was observed.

From Scheme 1, the proton-transfer rate constant k_{PT} can be estimated from the fluorescence quantum yields ratio (Φ'/Φ) of pyranine-adsorbed cationic LB films and time-resolved fluorescence spectra.[28]

$$(\Phi'/\Phi_0')/(\Phi/\Phi_0) = k_{PT}/(k_f + k_q) = k_{PT}\tau_o, \quad (4)$$

where Φ_0' and Φ_0 are the fluorescence quantum yields of protonated ($PyOH^*$) and deprotonated (PyO^{-*}) species, respectively, in absense of the proton-transfer reaction. Then, the following assumptions were made in order to determine k_{PT} in the adsorbed film. First, the fluorescence quantum yields of pyranine aqueous solutions at pH 0.6 ($PyOH^*$) and 10.2 (PyO^{-*}) were obtained in comparison to 1×10^{-5} mol L^{-1} quinine sulfate in 0.5 mol L^{-1} H_2SO_4 ($\Phi = 0.546$). Thus, the quantum yields ratio of the protonated (Φ_0)/deprotonated (Φ_0') was 1.72. Second, the spectrum of pyranine-adsorbed film was deconvoluted $PyOH^*$ and PyO^{-*} bands by using a gaussian function, and the Φ'/Φ was evaluated from their area ratio. Third, τ_o has a major contribution to the fluorescence lifetime of $PyOH^*$ band of the pyranine-adsorbed LB film. The results of the k_{PT} of pyranine-adsorbed films were 10 times faster than that of an aqueous solution ($\approx 10^{-9}$ s^{-1}). Thus, the pyranine molecule bound in the cationic LB film is located near the amino goup of octadecylamine as the proton acceptor, and these closer donor to the acceptor seems to cause the extremely rapid proton tansfer process. In terms of the film composition, it is evident that the disparity in the molecular microenvironment also affects the ESPT process. The difference in rate constant corresponds to the magnitude of the spectral shift in the absorption spectra. These results suggest that interaction among the pyranine molecules also affects the ESPT process. It is well known that the sulfonate goups as an electron-drawing substituent induce charge transfer from the lone pair of the oxygen to the aromatic rings and this charge transfer weakens the bond between the oxygen and hydrogen and enhance the proton mobility.[10] In the LB film with adsorbed pyranine, it is probable that the charge tansfer occurs not only beween the lone pair of the oxygen-aromatic ring-sulfonate group but also among the pyranine aggregate.

Conclusion

By using gemini cationic amphiphiles in additon to octadecylamine, the adsorption of pyranine molecules onto the cationic monolayers induced new monolayer properties and spectral changes. The visco-elasticity of the cationic monolayers corresponded to the spectral changes due to the difference in the dye orientation and packing in the monolayers. In addition, these facts were supported by the BAM images before and after adsorbing the pyranine molecules onto the cationic monolayers, which changed the surface pressure.

In these transferred films, the molecular arrangement of pyranine molecules was strongly affected by the film structure

and changed with the kinds of cationic film substances and composition. In particular, it was found that the ESPT rate constant in the LB films with adsorbed pyranine molecules was significantly greater than that in solution. These results can be ascribed to the molecular packing and orientation in the adsorbed-LB films.

The authors thank the NFT and MEIWA SHOJI Co., LTD for the observation of Brewster Angle Microscopy.

References

1 A. Ulman, *An Introduction to Ultra Organic Films*, Academic Press, New York, **1991**.

2 *Langmuir Blodgett Films*, ed. by G. Roberts, Plenum Press, New York, **1990**.

3 M. Takahashi, K. Kobayashi, K. Takaoka, T. Takada, K. Tajima, *Langmuir* **2000**, *16*, 6613.

4 T. Yoshimura, Y. Nagata, K. Esumi, *J. Colloid Interface Sci.* **2004**, *275*, 618.

5 K. Murali Mayya, A. Gole, N. Jain, S. Phadtate, D. Langevin, M. Sastry, *Langmuir* **2003**, *19*, 9147.

6 K. Ray, H. Nakahara, *Phys. Chem. Chem. Phys.* **2001**, *3*, 4784.

7 K. Ray, H. Nakahara, *J. Phys. Chem. B* **2002**, *106*, 92.

8 K. Ray, H. Nakahara, *Bull. Chem. Soc. Jpn.* **2002**, *75*, 1493.

9 M. Rini, B.-Z. Magnes, E. Pines, E. T. J. Nibbering, *Science* **2003**, *301*, 349.

10 T.-H. Tran-Thi, C. Prayer, P. Uznanski, J. T. Hynes, *J. Phys. Chem. A* **2002**, *106*, 2244.

11 K. Ray, H. Nakahara, *J. Photochem. Photobiol., A* **2005**, *173*, 75.

12 F. M. Menger, C. A. Littau, *J. Am. Chem. Soc.* **1993**, *115*, 10083.

13 G. L. Gaines, Jr., *Insoluble Monolayers at Liquid–Gas Interfaces*, John Wiley & Sons, Inc., New York, **1966**.

14 L. B. Hazell, A. A. Rizvi, I. S. Brown, S. Ainsworth, *Spectrochim. Acta, Part B* **1985**, *40*, 739.

15 M. Kasha, H. R. Rawls, M. A. El-Bayoumi, *Pure Appl. Chem.* **1965**, *11*, 371.

16 M. Murata, M. Villeneuve, H. Nakahara, *Chem. Phys. Lett.* **2005**, *405*, 416.

17 V. Czikkely, H. D. Föresterling, H. Kuhn, *Chem. Phys. Lett.* **1970**, *6*, 11.

18 I. R. Peterson, G. J. Russell, *Thin Solid Films* **1985**, *134*, 143.

19 A. Fujimori, Y. Sugita, H. Nakahara, E. Ito, M. Hara, N. Matsuie, K. Kanai, Y. Ouchi, K. Seki, *Chem. Phys. Lett.* **2004**, *387*, 345.

20 T. Förster, *Z. Elektrochem.* **1950**, *54*, 531.

21 A. Mironczyk, A. Jankowski, A. Chyla, A. Ozyhar, P. Dobryszycki, *J. Phys. Chem. A* **2004**, *108*, 5308.

22 Y. V. Il'chev, A. B. Demyashkevich, M. Kuzumin, H. J. Lemmetyinen, *J. Photochem. Photobiol., A* **1993**, *74*, 51.

23 P. Ballet, M. Van der Auwearer, F. C. De Schrever, H. Lemmetyinen, E. Vourimaa, *J. Phys. Chem.* **1996**, *100*, 13701.

24 L. Laguitton-Pasquier, M. Van der Auwearer, F. C. De Schrever, *Langmuir* **1998**, *14*, 5172.

25 N. Tamai, T. Yamazaki, I. Yamazaki, *Chem. Phys. Lett.* **1988**, *147*, 25.

26 P. Anfinrud, T. Causgrove, W. Sturve, *J. Phys. Chem.* **1986**, *90*, 5887.

27 M. I. Sluch, A. G. Vitukhnovsky, M. C. Petty, *Thin Solid Films* **1996**, *284–285*, 622.

28 S. V. Kombarova, Y. V. Il'ichev, *Langmuir* **2004**, *20*, 6158.

29 E. Pines, D. Huppet, N. Agmon, *J. Chem. Phys.* **1988**, *88*, 5620.